Department of Marine Technology - IMT

TMR4240 - Project Part 1

Marine Cybernetics

DP positioned supply vessel - Design and Control

Group:
Group 15

Authors:
Elias Strømmen Ravnestad
Mathias Netland Solheim
Johan Bakken Sørensen

September 28, 2020

Table of Contents

1 Introduction

This report details the work done for Part One of the semester project in the course TMR4240 Marine Control Systems I. The overall purpose of the project is to design and implement a dynamic positioning system for a supply vessel. The goal of Part One of the project is to design and validate the Current Velocity Model, DP Reference Model and the Controller for a supply vessel DP system.

The mathematical model of the vessel, with all equations of motion and corresponding hydrodynamic coefficients used in the simulations was provided in SIMULINK. A reference frame is presented in the report and used in the simulations. Theory behind process plant modelling and control plant modelling is provided. A control plant model for the vessel, to be used in design of an eventual observer, is proposed in mathematical terms. The reference model implemented in the simulations is presented. A controller is chosen and implemented. To achieve optimal DP functionality the controller is fine tuned.

To verify the functionality of the implemented systems several simulations were run in four different scenarios. Each scenario consisted of typical DP-positioning operations, such as station-keeping under environmental loads, small set-point variation in position and orientation and finally a classic box-test, which test the systems ability to maneuver to and stabilize around four different set-point, changing both position and heading references.

2 Theory

2.1 Reference Frame

As a reference frame for the vessels motions, the North-East-Down- (NED), and body-fixed frame were used.

The NED-frame is a tangent plane to the earths surface and is denoted as:

$$\{n\} = [x_n, y_n, z_n]^T$$

where x_n follows true north, y_n follows east and z_n is positive pointing downwards. The body-fixed frame is corresponds to the vessels different directions and is denoted as:

$$\{b\} = [x_b, y_b, z_b]^T$$

where x_b corresponds to the vessels longitudinal direction, y_b corresponds to transverse directions and z_b points in a direction normal to x_b and y_b.

2.2 Process Plant Model

The process plant model, or simulation model, is a mathematical model of the physical process. In the case of a supply vessel there is a desire to simulate the real world dynamics. The process plant model gives the necessary detailed descriptions of the vessels dynamics as well as external forces and moments from thrusters and environmental loads.

2.2.1 Vessel Dynamics

When modeling vessel dynamics, it is common to separate the total model into two components using superposition. The first is a wave-frequency model and the second is a low-frequency model, hereby referred to as WF- and LF-model respectively. Thus, the total motion becomes a sum of the WF- and LF-models.

The WF-motions are caused by first order wave loads, while the LF-motions are assumed to be the result of second-order mean and slowly varying wave loads, current loads, wind loads, and thrust forces.

2.2.2 Low-frequency Process Plant Model

In the lecture slides the nonlinear LF process plant model for a 6 DOF DP system is expressed by equation 2.1.

$$M\dot{v} + C_{RB}(v)v + C_A(v_r)v_r + D(v_r) + G(\eta) = \tau_{wind} + \tau_{wave2} + \tau_{thrust} \tag{2.1}$$

Where M is the mass matrix, including low frequency added mass coefficients. $C_{RB}(v)$ and $C_A(v_r)$ are the Coriolis matrix for respectively rigid body motion and added mass. $D(v_r)$ is the linear and nonlinear damping matrix and $G(\eta)$ is the restoring force matrix. τ_{wind} and τ_{wave2} is wind forces and second order wave forces(mean and slowly varying). The τ_{thrust} are the thrust forces. In case of ice and mooring it is possible to add τ_{ice} and $\tau_{mooring}$, on the right side of the equation. v is the speed of the vessel. The relative velocity vector is defined by equation 2.2.

$$v_r = [u - u_c, v - v_c, w, p, q, r]^T \tag{2.2}$$

Where u is the speed in surge and u_c is current the speed in surge, v is the speed in sway and v_c is the current speed in sway, w is the speed in heave, and p, q, and r are the angular speed in respectively roll, pitch and yaw.

2.2.3 Wave-frequency Process Plant Model

The behavior of first order linear waves is solved as two separate sub-problems, wave reaction and wave excitation. Which is respectively forces due to the vessel being forced to oscillate with the waves and forces due to the vessel being restrained from oscillation. The lecture notes (Sørensen [2018]) express the solution to the respective problems by equation 2.4 and equation 2.3.

$$M(\omega)\ddot{\eta}_{Rw} + D_p(\omega)\dot{\eta}_{Rw} + G\eta_{Rw} = \tau_{wave1} \tag{2.3}$$

$$\eta_w = J(\bar{\eta}_2)\dot{\eta_{Rw}} \tag{2.4}$$

Where

$$\bar{\eta}_2 = [0, 0, \psi_d]^T \tag{2.5}$$

Where ψ_d is the heading. $M(\omega)$ is the inertia matrix, including frequency dependent added mass coefficients. η_{Rw} is the WF motion vector in the hydrodynamic frame. η_w is the earth fixed wave induced position. $D_p(\omega)$ is the wave radiation damping matrix. G is the linearized restoring coefficient matrix. τ_{wave1} is the first order wave excitation vector and the J is the rotation matrix.

2.3 Control Plant Model

In DP systems it may not be possible or too expensive to measure many of the states of interest concerning control. Therefore there is an desire to calculate or reconstruct those states based on the measurements available. This is called state estimation and is done in the observers. An observer also provides filters for noise and wave induced motions such that only the LF states affect the controller. The red line in Figure 2.1 provides an example of how an observer uses a low pass filter to remove high frequencies and a notch filter to remove resonance. In order to compute a state estimation, it is necessary to implement a control plant model. A control plant model is a simplified mathematical model of the vessel. The control plant model will be used in construction and design of the observers. The observer should also be able to handle temporary loss of position and heading measurements by estimating the motion in the feedback loop.

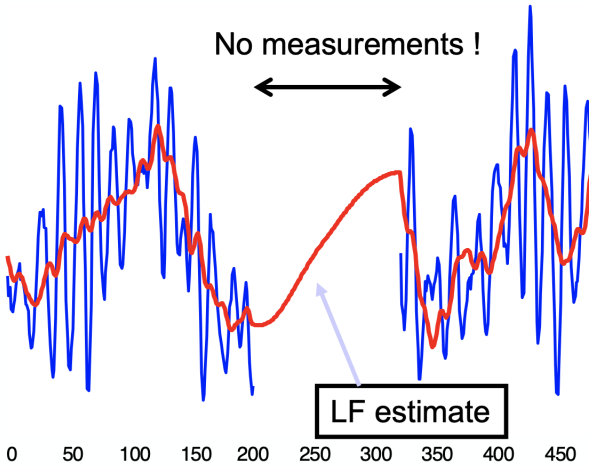

Figure 2.1: Dead reckoning(Lecture slides: DP Control CPM)

This kind of state estimation is called dead reckoning, see Figure 2.1. Dead reckoning allows increased operability by fault-tolerant control and smooth transitions to the actual position and heading when signals come back.

2.3.1 Low-frequency Control Plant Model

A LF control plant model is a simplified model of the actual LF process plant model, equation 2.1. In the case of a supply vessel, the first step of simplifying is reducing degrees of freedom, from a 6 DOF system to a 3 DOF system. This is done by using model reduction matrices,$H_{i \cdot j}$, that reduces the degrees of freedom considered in the matrices in the equation, $M, C_{RB}(v), C_A(v_r), D(v_r)$ and $G(\eta)$. Next step is assuming small velocities, v_r and linearity. Then the Coriolis components can be neglected, reducing the equation 2.1 into equation 2.6.

$$M\dot{v} + Dv + R^T(\psi)G\eta = \tau + R^T(\psi)b \tag{2.6}$$

Where

$$\dot{\eta} = R(\psi)v \tag{2.7}$$

and

$$R(\psi) = \begin{pmatrix} cos(\psi) & -sin(\psi) & 0 \\ sin(\psi) & cos(\psi) & 0 \\ 0 & 0 & 1 \end{pmatrix} \tag{2.8}$$

and the new velocity vector becomes

$$v = [u, v, r]^T \tag{2.9}$$

This system is linear, except for the kinematics represented by $R(\psi)$. The $G \cdot \eta$ component represents mooring, and can therefore be removed from the equation in this case. The b term is the bias model. The bias model represents slowly varying excitation loads due to wind, current and second order waves, and take care of unmodeled dynamics. The bias model contributes with an integral effect, which contradicts steady state deviations. In the observer there are two different commonly used bias models, the first order Markov model, equation 2.10, and the Wiener process, equation 2.11.

$$\dot{b} = -T_b^{-1} b + E_b w_b \tag{2.10}$$

$$\dot{b} = E_b w_b \tag{2.11}$$

w_b is a zero-mean Gaussian white noise vector, T_b is a diagonal matrix of the bias time constants, and E_b is a diagonal scaling matrix. Equation 2.11 will be used further in this report.

2.3.2 Wave-frequency Control Plant Model

In order to create a simplified model of the WF individual motions, it is not necessary to make as much of assumptions and simplifications as for the LF model. The WF model can fully be represented by a harmonic oscillator, written in state space form, equation 2.12 and equation 2.13.

$$\dot{\zeta}_w = A_w \zeta_w + E_w w_w \tag{2.12}$$

$$\eta_w = C_w \zeta_w \tag{2.13}$$

$\dot{\zeta}_w$ is the wave induced motion vector, A_w is the system matrix, E_w is the disturbance matrix, w_w is a zero-mean Gaussian white noise vector and C_w is the measurement matrix. All these matrices are defined in Sørensen.

2.3.3 Complete Control Plant Model

The proposed complete control plant model for a supply ship is

Low-frequency model:

$$M\dot{v} = \tau + R^T(\psi) b - Dv \tag{2.14}$$

Bias model:

$$\dot{b} = E_b w_b \tag{2.15}$$

Kinematics:

$$\dot{\eta} = R(\psi)v \tag{2.16}$$

Wave frequency model:

$$\dot{\zeta}_w = A_w \zeta_w + E_w w_w \tag{2.17}$$

$$\eta_w = C_w \zeta_w \tag{2.18}$$

Measurements:

$$y = \eta + \eta_w + v \tag{2.19}$$

Where the v is the measurement noise term.

3 Current Model

In order to achieve a realistic situation with environmental loads affecting the process plant, a current model is implemented. This is a mathematical model applying a disturbance to the vessel similar to that of a surface current in the real world. The current model used can be modeled in the NED-frame as shown in Equation 3.1

$$\nu_c = \left[V_c \cos(\psi_c), V_c \sin(\psi_c)\right]^\top \tag{3.1}$$

Where ν_c is the current velocity in NED-frame, V_c is the current velocity amplitude, and ψ_c is the current direction, expressed as an angle in the NED-frame. A more realistic model features a variation in the current velocity amplitude V_c expressed with a Gauss-Markov process, as shown in Equation 3.2

$$\dot{V}_c + \mu V_c = w \tag{3.2}$$

Where w is Gaussian white noise, and μ is a positive constant. This causes the current velocity to vary slightly, but not suddenly over time, akin to a realistic current variation. This was not implemented in Part 1, since the simulations specified a constant velocity. It may however become relevant for study in Part 2 of the project.

3.1 Implementation

The current model was implemented in Simulink using a pre-defined block from the MSS toolbox, which receives an angle ψ_c and a current velocity V_c, and applies the mathematical model in Equation 3.1.

Two cases, for Simulation 1 and 2, were implemented and separated by a switch, such that both simulations could be run without changing the model itself. For the second case, a linearly varying current direction was to be implemented. It was said to linearly vary between 180° and 270°. No other parameters for the variation was specified, so in this case it was set to have a starting angle at 180°, rising to 270° over 5 minutes before remaining at this level. This was achieved using a ramp and saturation block. The current model is shown in Figure 3.1, where the MSS North-East current block is used, before the signal is converted to the body frame of the ship.

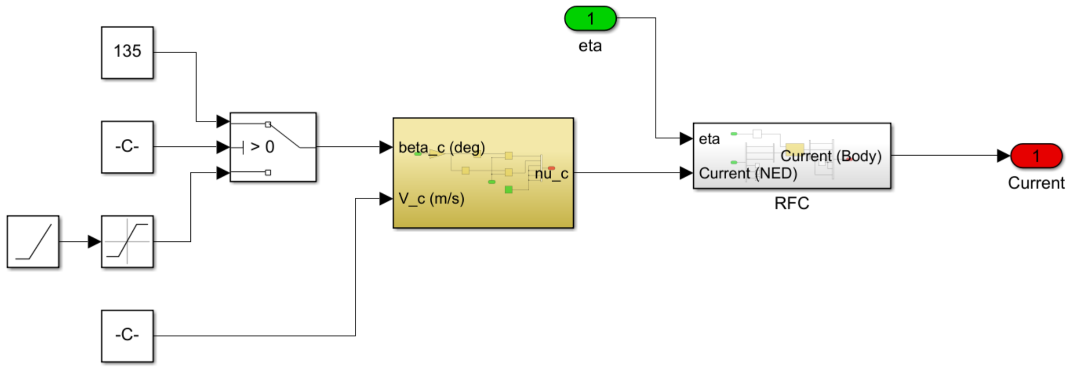

Figure 3.1: Current model in Simulink

4 Reference Model

When an operator designates a new set-point for a vessel, the distance might be considerable. This means that the deviation becomes quite large, causing the forces generated by the vessels actuators to become saturated. This results in large accelerations causing sudden motions of a higher magnitude than desired. Working in saturation can also cause instabilities in the system, especially for integrators.

To compensate for this we want to implement a method to generate a trajectory between two set points. This is the reference model. Its purpose is to synthesize the desired position, velocity, and acceleration from set points, and feed these filtered global set-points into the control-algorithm. The result is a much smoother transition between set points.

4.1 Implementation

For this project a third-order filter as described in the lecture notes (Sørensen [2018]) and in Fossen [2011], is implemented as the reference model. The "Position and Attitude Reference Model", as Fossen refers to it as, is composed of a low-pass filter cascaded with a mass-damper-spring system. The transfer-function between the set-point position η and reference-value r is described in equation 4.1:

$$\frac{\eta_{d_i}}{r_i} = \frac{1}{1+Ts}\frac{\omega_{n_i}^2}{s^2+2\zeta_i\omega_{n_i}s+\omega_{n_i}^2} = \frac{\omega_{n_i}}{\omega_{n_i}+s}\frac{\omega_{n_i}^2}{s^2+2\zeta_i\omega_{n_i}s+\omega_{n_i}^2}, \quad i=1,2,3 \tag{4.1}$$

In equation 4.1 the relation of $T = 1/\omega_n$ is used. The reference model is implemented as its own subsystem in Simulink:

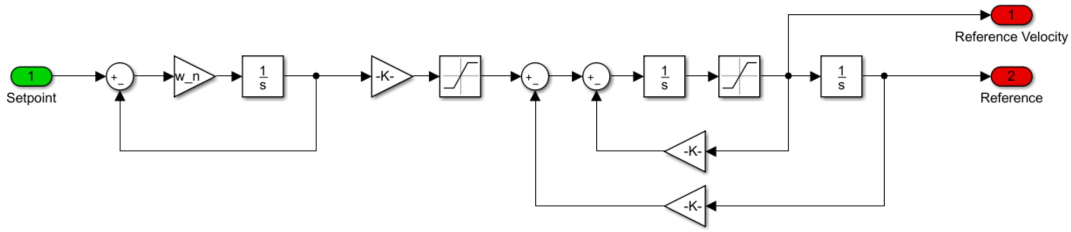

Figure 4.1: Implementation of Reference model in Simulink

To prevent the reference model from feeding unfeasible references to the controller, saturation was implemented on the acceleration- and velocity-terms.

4.2 Tuning

The reference model contains six variables that must be tuned for the system to function optimally. These consist of the damping ratio ζ_i and the natural frequency ω_{n_i}, each in all three degrees of motion.

The tuned damping ratios are presented in equation 4.2.

$$\zeta_i = \begin{bmatrix} 1 & 1 & 1 \end{bmatrix}^T \tag{4.2}$$

for all degrees of motion, as it was proved that a critically damped system was easy to work with. It provided reasonably fast and accurate response.

The reference systems bandwidth needs to be lower than that of the motion control system. To tune the reference system we found the actual vessels natural frequencies, and identified the lowest one. This was taken as a starting point, and tuned downwards.

When tuning, a couple of protocols were followed: Considering the supply ships natural shape, it is clear that the vessels maneuverability is much better in longitudinal direction, than in the lateral. It is therefore reasonable to tune in a more aggressive behaviour, i.e higher *omega*, in surge than in sway.

It is also desirable to keep the heading of the ship as stable as possible, so the ω_3 was tuned with the least aggressive behaviour. Thus the parameters were tuned after the following relationship $\omega_1 > \omega_2 > \omega_3$. The final parameters are presented in equation 4.3.

$$\omega_{n_i} = \begin{bmatrix} 0.08 & 0.04 & 0.03 \end{bmatrix}^T \tag{4.3}$$

The parameters in equation 4.2 and equation 4.3 resulted in the desired behaviour; a smooth trajectory between set points.

5 Controller Design

The purpose of the controller is to achieve correspondence between the state variables and the desired setpoint. In this case, the controller achieves this by use of the feedback-loop. By comparing the current state of the control plant with the desired state, it generates an input to the control plant in order to reduce the difference between state and setpoint.

In this case, the controller receives a desired trajectory for the ship, given by the reference model. In addition; it receives the current value of the state variables we wish to control, the surge, sway and yaw, as well as their rates of change. The algorithm inside then generates a control plant input τ, which is fed into the ship model, after correcting for the reference frame.

5.1 Control Algorithm

The control algorithm decides how the deviation between state and setpoint are manipulated in order to give a good input to the control plant. Some different control algorithms were considered, such as the *Linear Quadratic Regulator* (LQR) algorithm. In the end, the standard Proportional-Integral-Derivative, or PID-algorithm, was chosen. The PID-controller was chosen due to its relatively easy implementation and usage, as well as the group members' familiarity with its behaviour.

The PID-algorithm can be expressed mathematically as in Equation 5.1. It manipulates the deviation in three different way. The proportional part adds an output directly proportional to the deviation. The integral part will apply an output based on all previous deviation, and can be thought of as a long-term corrector. The derivative part will generate a controller output based on how the deviation changes in that moment, and can therefore be thought of as a predictor.

$$u(t) = K_p e(t) + K_i \int_0^t e(t')dt' + K_d \frac{de(t)}{dt} \tag{5.1}$$

In Equation 5.1, $u(t)$ is the controller output/control plant input, and $e(t) = \eta_0 - \eta_{now}$ is the deviation between set-point and current position. The controller gains K_p, K_i and K_d are all constants, and determine the effect of each part. These constants can be evaluated by tuning the control system.

5.2 Implementation

The Simulink model for the controller is shown in Figure 5.1. In addition to performing the PID-algorithm, it also converts from the NED reference frame that the setpoint is specified in, into the body frame of the ship. The incoming signal ν, which represents the rates of change in surge, sway and yaw, has a desired state of $\mathbf{0}$ (no change in position/heading) and is thus fed directly in as a deviation.

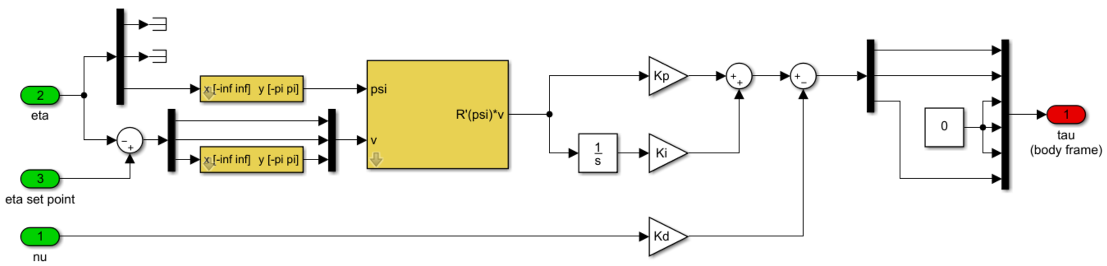

Figure 5.1: PID-controller implemented in Simulink

5.3 Tuning

Different values for the controller gains will yield different types of behaviour from the system. Some sets of constants will cause a calm and steady convergence to the setpoint, whilst others might cause overshoot and/or oscillatory behaviour. Some combinations of controller gains might destabilize the system altogether. There are a multitude of tuning methods to find a decent set of controller gains. For this project, a tuning scheme from Fossen [2011] was used.

5.3.1 Tuning by Fossen's algorithm

The tuning scheme starts by assuming a reasonable bandwidth for the control plant, as well as a damping ratio, which will determine the shape of the response. For the damping ratio, a value of 1 was chosen, as this would yield a response similar to that of a critically damped mass-spring-damper system. For the bandwidth, Fossen [2011] specifies that a value of 0.01 is reasonable for large tankers, whilst a value of 0.1 was suitable for smaller vessels. A value of 0.1 was chosen to go on with for now.

From the bandwidth ω_b and a damping ratio ζ a natural frequency can be determined by Equation 5.2

$$\omega_n = \frac{1}{1 - 2\zeta^2 + \sqrt{4\zeta^4 - 4\zeta^2 + 2}} \omega_b \tag{5.2}$$

Together with the mass m, one can then find the gain constants by the following scheme

Table 5.1: Gain constants by Fossen's algorithm

K_p	$m\omega_n^2$
K_i	$\frac{1}{10}\omega_n K_p$
K_d	$2\zeta\omega_n m$

The constants produced by this algorithm were applied to the Simulink model. Because the algorithm is based for single-input single-ouput (SISO) systems, the same constants were applied to correct all three degrees of freedom (surge, sway, yaw). With this in mind, optimal controller behaviour was not expected. The gain constants turned out to be quite a bit lower than what was needed, especially in yaw. The controller gains from the Fossen algorithm did however serve as a decent benchmark from which manual testing could be applied to find a better tuning result.

5.3.2 Manual tuning

Starting out with the suboptimal result from the Fossen algorithm, it was decided to attempt manual tuning to improve the performance. A PID-controller is relatively easy to tune, since each gain value has a clear response behaviour associated with it. Thus, the manual tuning process yielded some decent insights into the system's dynamics.

After some back and forth manual tuning attempts, the gain constants presented in Table 5.2 were the final values. These are by no means final numbers, and will likely be further changed around as the project develops. The constants were chosen to ensure a decent performance on all the four simulations that were conducted for Part 1.

Table 5.2: Controller gain constants

	Surge	**Sway**	**Yaw**
K_p	$5e+5$	$5e+5$	$2e+7$
K_d	$1e+7$	$1e+7$	$2e+8$
K_i	$1e+2$	$3e+3$	$1e+2$

6 Simulation Results

6.1 Simulation 1: Station-keeping under current loads

The first simulation tested the DP capabilities of our system. In this scenario, the vessel is under load from a current moving southeast at a velocity of $V_c = 0.5[m/s]$. The mission is to maintain the same position under the environmental loads. The set-point is therefore defined to $\eta_{ref} = \begin{bmatrix} 0 & 0 & 0 \end{bmatrix}^T$ The southeast current direction is interpreted as a angle of $135°$

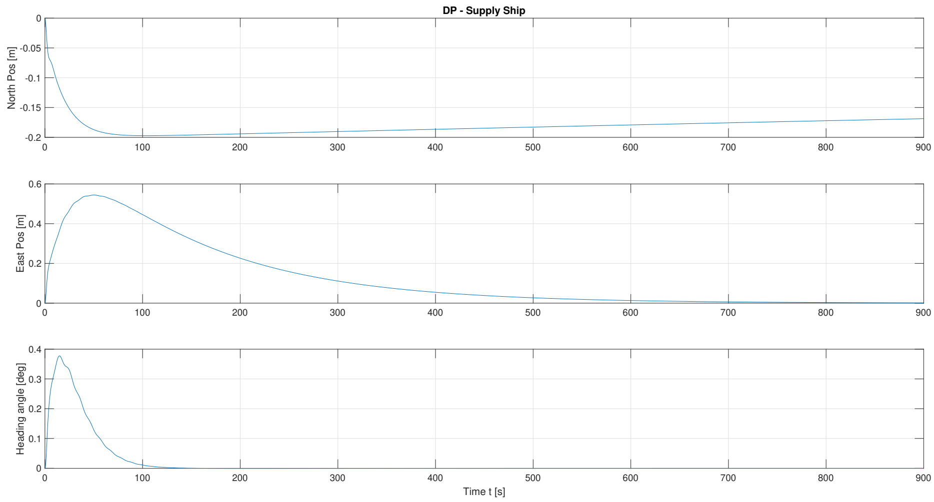

Figure 6.1: North, East, and heading under constant current direction

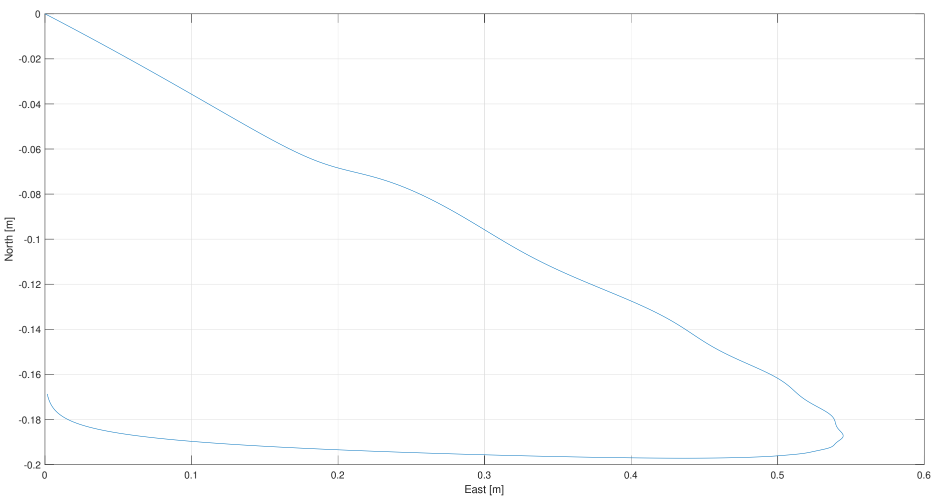

Figure 6.2: North-East position under constant current direction

6.2 Simulation 2: Station-keeping under varying current directions

To further test the robustness of our controller, we introduce a current varying in direction. As opposed to the current in 6.1, which came in at a constant angle, the current angle now varies linearly from north to east at the same velocity. The mission is still to maintain the same position under the environmental loads. The set-point is thus also still $\eta_{ref} = [\ 0 \quad 0 \quad 0\ ]^T$.

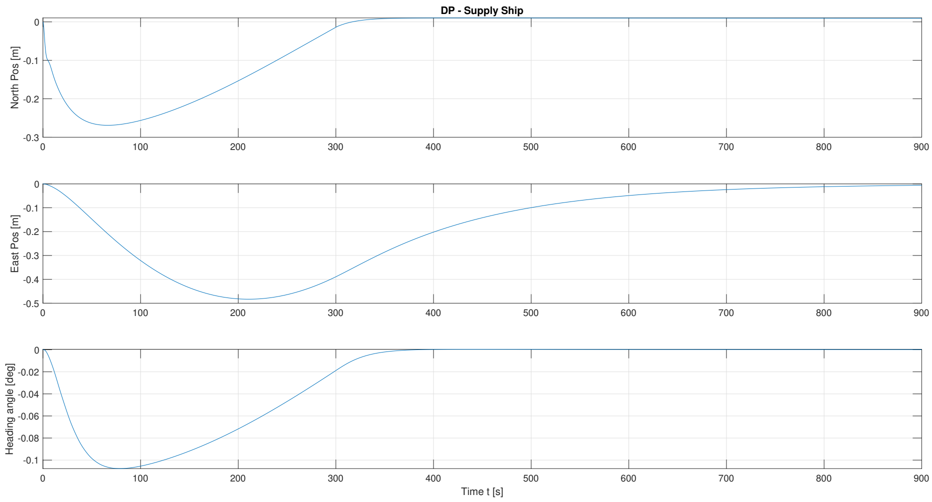

Figure 6.3: North, East, and heading under varying current direction

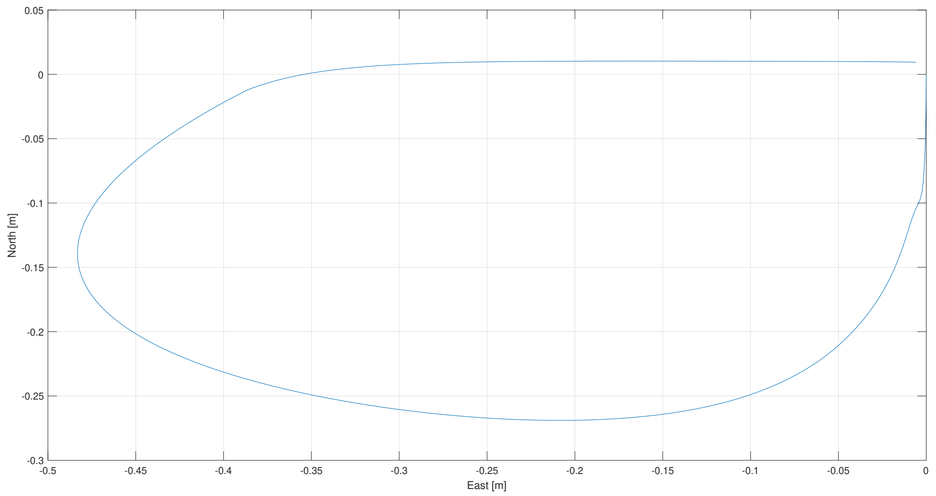

Figure 6.4: North-East position under varying current-direction

6.3 Simulation 3: Navigation with and without Reference Model

The next simulation tests the refrence models capabilities. The vessel is given the set-point of $\eta_{ref} = [\ 10 \quad 10 \quad \frac{3\pi}{2}\ ]$, and made to maneuver there, first without a reference model, then with it. The simulations are to be carried out without a current-load.

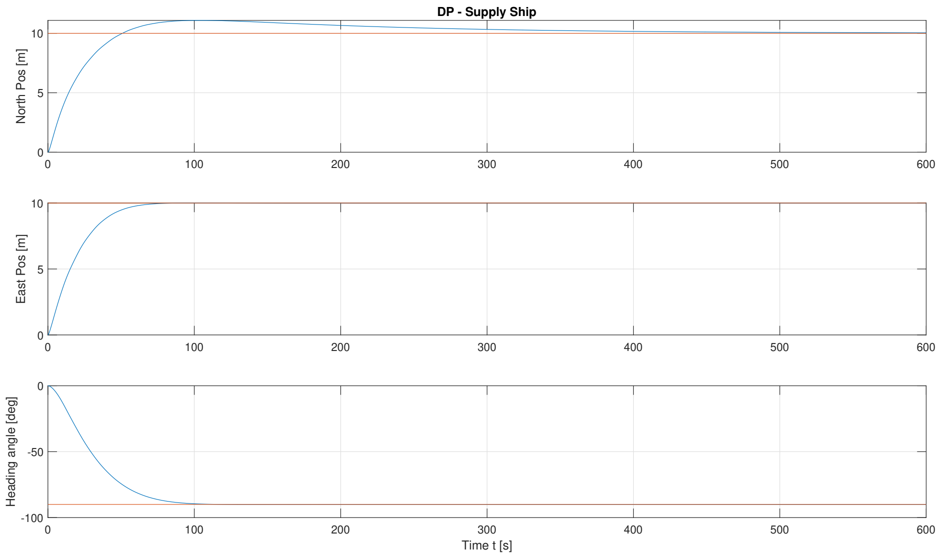

Figure 6.5: North, East, and heading during setpoint maneuver - No reference model

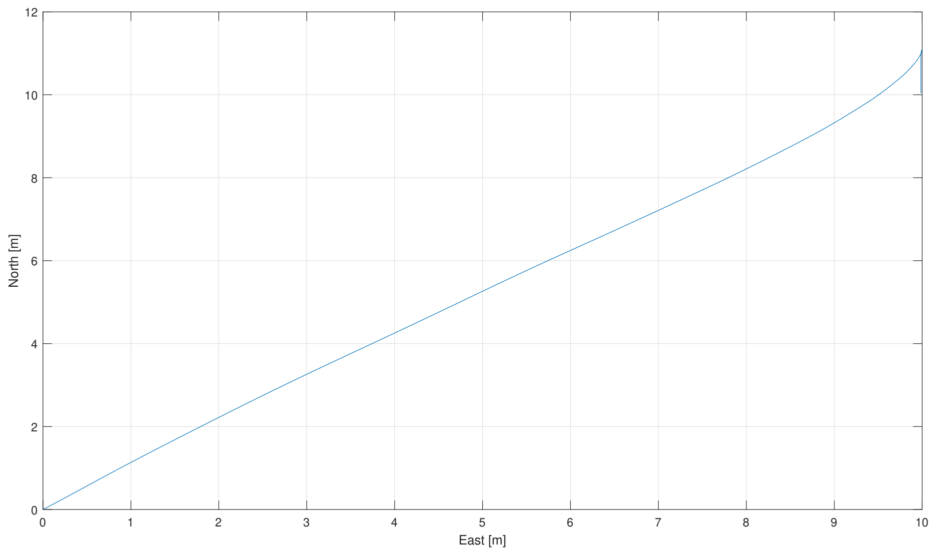

Figure 6.6: North-East position during setpoint maneuver - No reference model

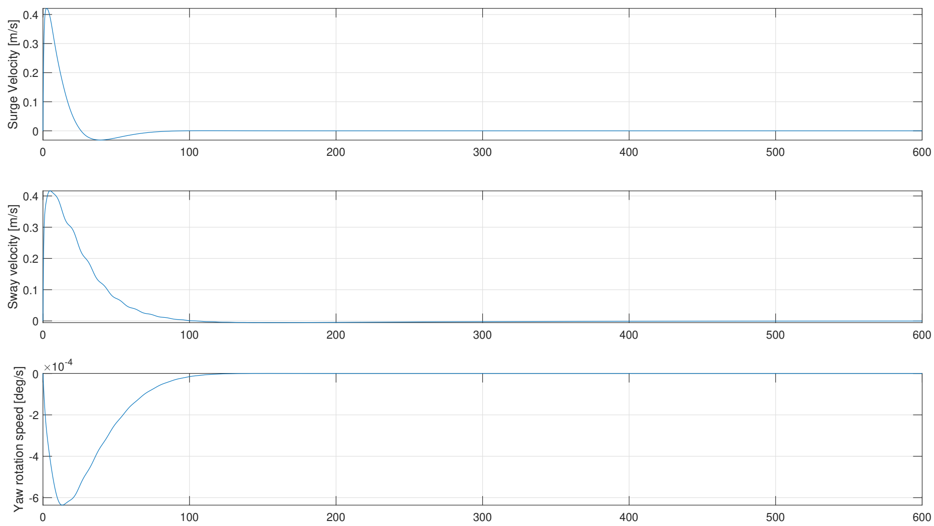

Figure 6.7: Velocity in surge, sway and yaw during setpoint maneuver - No reference model

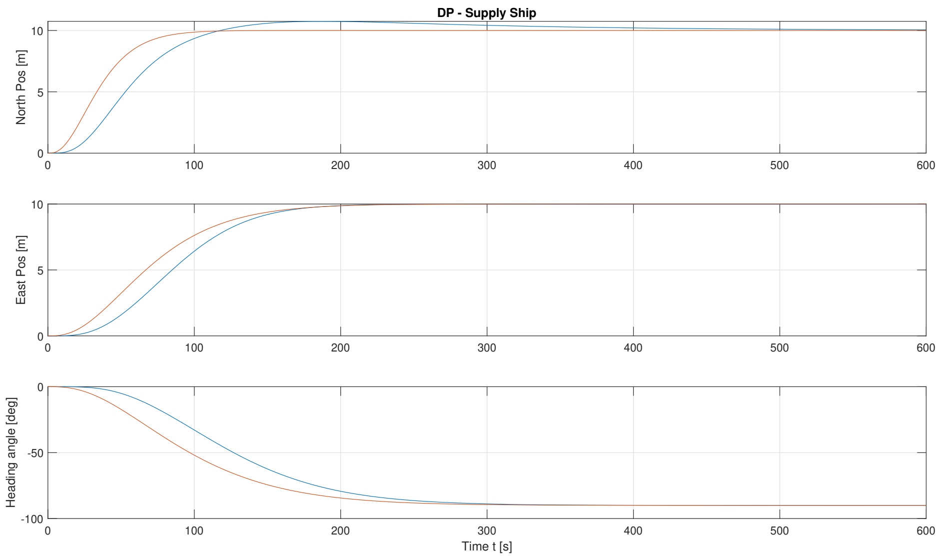

Figure 6.8: North, East, and heading during setpoint maneuver - Reference model

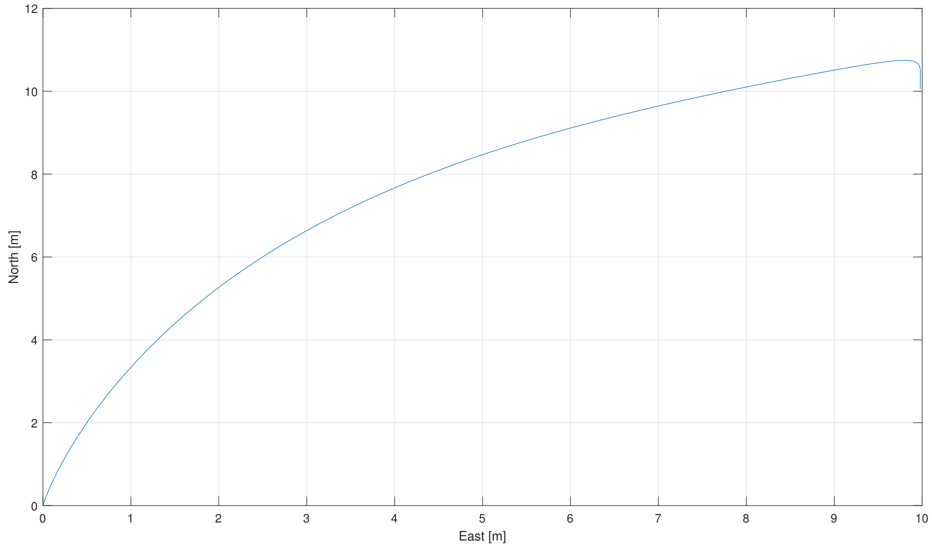

Figure 6.9: North-East position during setpoint maneuver - Reference model

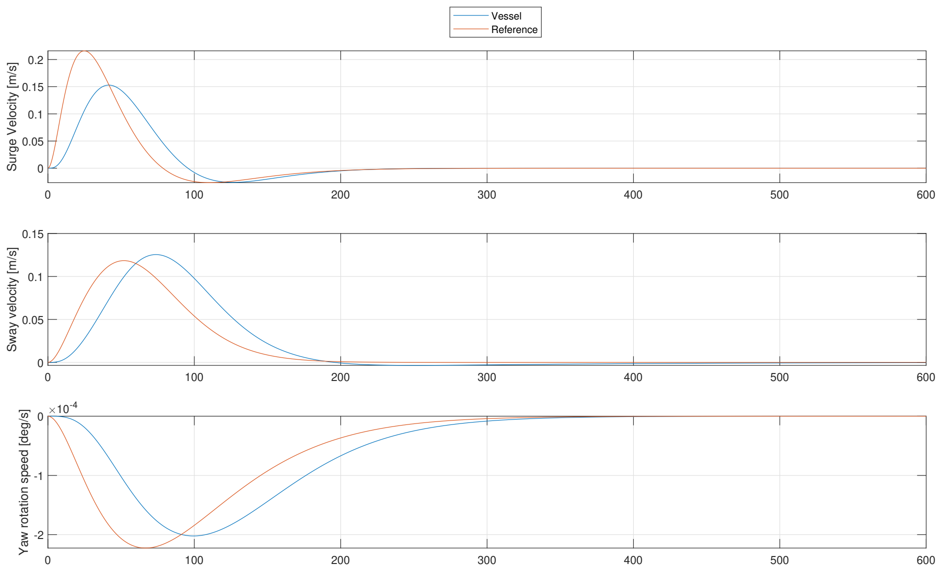

Figure 6.10: Velocity in surge, sway and yaw during setpoint maneuver - Reference model

6.4 Simulation 4: 4 corner test

The final tests consists of a DP four corner test. The vessel must pass through four set-points in a square pattern, keeping a steady state in each before moving on. The order is presented in table 6.1

The simulation is to be run in without environmental forces, and truly tests the robustness of the DP system.

Set-point	North	East	Heading
η_0	0	0	0
η_1	50	0	0
η_2	50	-50	0
η_3	50	-50	$-\frac{\pi}{4}$
η_4	0	-50	$-\frac{\pi}{4}$
η_5	0	0	0

Table 6.1: Order of set-points

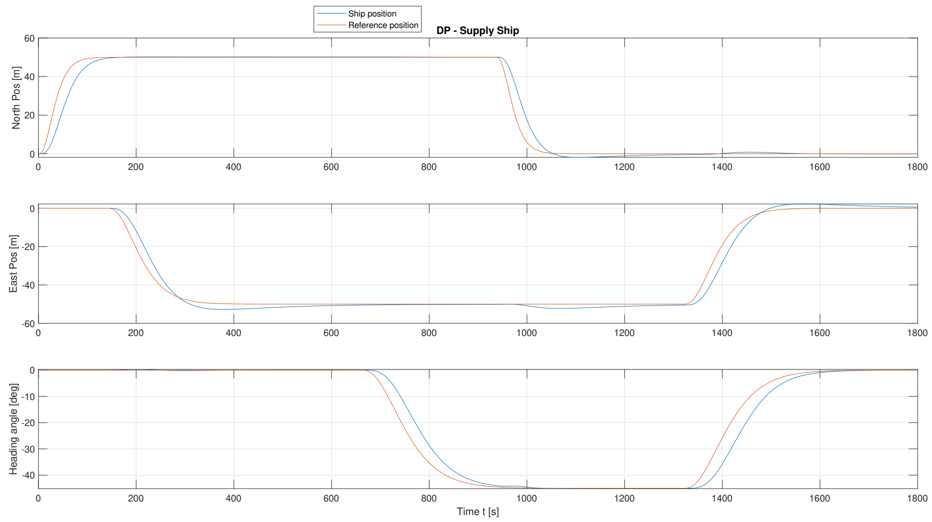

Figure 6.11: North, East, and heading - Four corner test

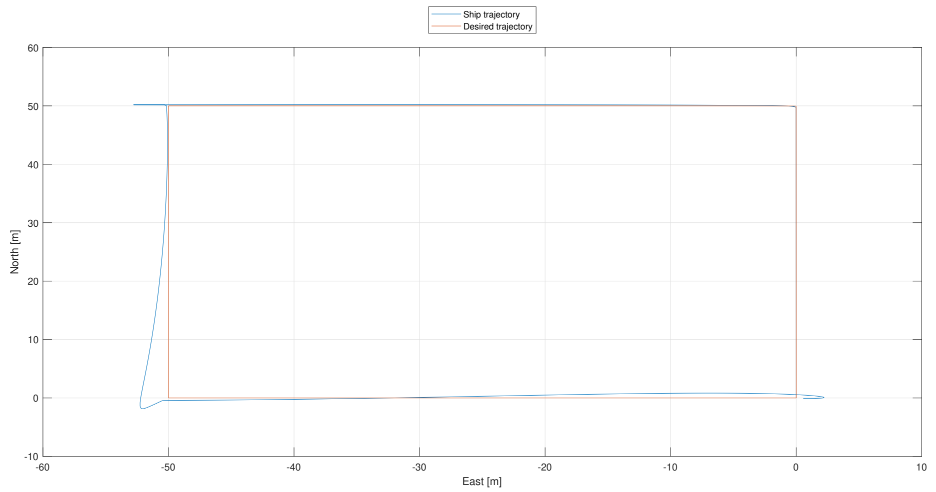

Figure 6.12: North-East position during setpoint maneuver - Four corner test

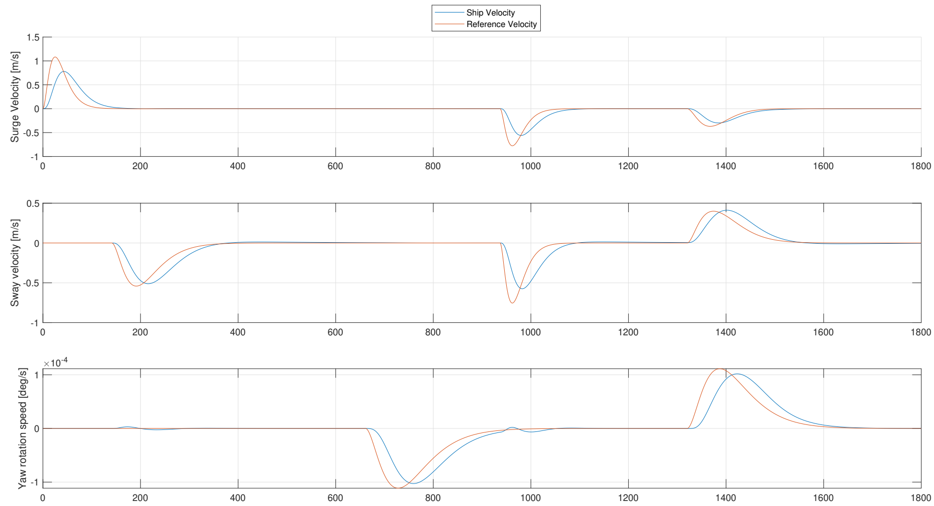

Figure 6.13: Velocity in surge, sway and yaw during setpoint maneuver - Four corner test

7 Discussion

7.1 Simulation 1

As can be observed from figure 6.2, the current causes the vessel to drift slightly to the south east. In total the ship drifts about 0.5 m to the east and 0.20 m to the south before the system completely counters the current. This takes a around 50 seconds, in both north and east direction.

Part of the mission was to achieve a "steady state" for the vessel. When one looks at the figures for north position, it might seem like the steady state is not achieved due to the fact that the north position had not fully converged towards a fixed value, like east-position and the heading have.

At the current state the controller seems to react slowly in surge and sway, taking almost 700 seconds to reach steady state in sway, and never fully reaching steady state in surge. This is a matter of tuning the system, specifically the proportional and integral gains in surge and sway respectively.

When we took the ships dimensions into consideration, the displacement seem within a margin of error. With an $Lpp = 82.8[m]$, an error of 20 cm can be considered insignificant. We therefore consider it to be a reasonable result for now, but the system must be more carefully tuned for the next part, especially towards a faster response.

7.2 Simulation 2

Looking at Figure 6.4 we can see that the ship follows the current southbound, but manages to counter this movement within 0.25m. As the current pulls the ship westward, the DP-system counters the movement before half a meter has been traversed. The ship then follows a calm trajectory toward the start point.

The North position looks a little incorrect, however. We can see this most clearly in Figure 6.4, where the trajectory is a little off the line indicating zero North position. However, this error is in the centimeter range, and probably not something of great concern for a vessel this size.

The heading sees little change at all, barely a tenth of a degree out of position, and this is quickly mitigated by the controller as seen in Figure 6.3. While some positional discrepancies are observed in the North and East position, these aren't of significant size. We can also see in Figure 6.3 that the East position spends a longer time adjusting itself than the north position, this is likely because the controller needs some time to adjust to the varying current, that has an increasing contribution in this direction.

7.3 Simulation 3

When comparing figures 6.7 and 6.10, along with figures 6.5 and 6.8, the effects of the reference model are clear. The vessels velocity and acceleration-plots follow a smoother and less aggressive approach. This results in the smoother trajectories that can be observed in figure 6.8. It is clear that the reference model is working as intended.

One thing to note is the overshoot in surge. This is not ideal, and another symptom that must be treated with tuning. The integral-gain is the most likely culprit, causing slight integral-windup. The solution would be to decrease the integral-gain in surge.

7.4 Simulation 4

We observe from Figure 6.12 that the first trip goes by quite smoothly, with the ship heading straight north, slowing down and turning the corner with little problems. It then seems to get too eager, overshooting on its way to the second corner, and has to readjust itself before continuing. This overshoot is quite large, encompassing at least a few meters, and we can see in Figure 6.11 that it spends quite a bit of time correcting itself. This is of course not optimal, and might correlate to the drift in east position we observe on the journey towards the third corner, because of a saturated integral correction due to the long time spent out of position.

The approach to the third corner goes more smoothly than to the second, and a faster correction can be seen in Figure 6.11. Approaching the fourth and final corner, we observe yet another slight overshoot. The overshoots might indicate that some more precise tuning is required to better adjust for this simulation test. The system still performs well, and the paths of the ship follow the reference with a decent margin.

The heading can be seen in Figure 6.11 to spend quite some time adjusting itself, but is by far the most well behaved of the bunch. It follows the reference quite well, with some slight delay, but a smooth trajectory and nice shape.

Similarly to the heading value, the velocity trajectories can all be seen as slightly delayed responses to the reference velocities, as can be seen in Figure 6.13. The velocities also look reasonable, barely ever exceeding 1m/s in both surge and sway, so there are no sudden large velocity spikes on the ship.

All in all, the corner test is not perfect, but it does show the strengths and weaknesses of the system, and opens up for improvements in Part 2. We see that the system follows up well on the reference model, and largely sticks to the desired trajectory, albeit with some deviations here and there. While not catastrophic, it is desirable with less discrepancies in the finished DP-system.

8 Conclusion

Based on the mathematical model of the vessel provided in SIMULINK, a DP system model was created and simulated. Based on theory a suitable reference frame were chosen, the physical system of the ship were modelled in a process plant model, and a simplified model of the process plant were proposed as control plant model. A current model and a reference model were chosen and implemented in order to respectively simulate the effects of the current on the vessel and to generate a trajectory between two set points. A PID-controller were chosen as DP-controller, and tuned using first using Fossens algorithm, then manually. Simulations were ran proving that the reference model works as intended. The controller however seems in need of more fine tuning. While its response are not to far of ideal, it needs to respond faster in surge and sway, along with eliminating overshoot in surge. For fix the issues, we would propose to alter the proportional and integral gains in surge and sway.

In conclusion, the system seems to be in need of slightly more tuning in surge and sway, while the reference model and current model were implemented succesfully.

Bibliography

Thor I. Fossen. *Handbook of Marine Craft Hydrodynamics and Motion Control*. John Wiley & Sons, Ltd, 2011.

Asgeir J. Sørensen. *Marine Cybernetics towards Autonomous Marine Operations and Systems - Lecture Notes*. Department of Marine Technology, NTNU, 2018.